Thermo-compositional convection in Europa's icy shell with salinity

Lijie Han[1,2] and Adam P. Showman[1]

Received 6 July 2005; revised 7 September 2005; accepted 19 September 2005; published 19 October 2005.

[1] We present two-dimensional numerical simulations of thermo-compositional convection to test the hypothesis that the combined buoyancy from both thermal and salinity contrasts in Europa's ice shell can produce the numerous uplifts and pits on Europa's surface. Our simulations show that uplifts and pits with amplitude of 100–500 m and diameters of 10–30 km (similar to some of the observed features) can be produced in a 10–30 km-thick ice shell with 2–10% compositional density variations if the viscosity contrast due to temperature variation does not exceed 10^6. The pit and uplift formation time and lifetime are approximately proportional to the surface viscosity, ranging from 10^4 years to 10^7 years for viscosity contrasts of 10^4–10^6. Convection cannot produce substantial surface topography if the viscosity contrast exceeds 10^7–10^8. These results imply that thermo-compositional convection can only produce Europa's pits and uplifts if Europa's surface is weak. **Citation:** Han, L., and A. P. Showman (2005), Thermo-compositional convection in Europa's icy shell with salinity, *Geophys. Res. Lett.*, *32*, L20201, doi:10.1029/2005GL023979.

1. Introduction

[2] Europa's surface is distributed with chaos and numerous small (3–30 km-diameter) pits, uplifts, and irregularly shaped landforms [*Pappalardo et al.*, 1998; *Greeley et al.*, 1998; *Riley et al.*, 2000; *Greenberg et al.*, 2003]. Many authors have proposed that pits, domes, and chaos resulted from solid-state convection in the ice shell, perhaps aided by partial melting [*Pappalardo et al.*, 1998; *Rathbun et al.*, 1998; *Head and Pappalardo*, 1999; *Collins et al.*, 2000; *Sotin et al.*, 2002; *Nimmo and Manga*, 2002]. However, numerical simulations of thermal convection have shown that the uplifted topography produced in the models is far less than the observed heights [*Showman and Han*, 2004, 2005].

[3] Evidence suggests that salts are present on Europa's surface. Galileo NIMS sensed the top few microns of Europa's surface and found non-water-ice materials concentrated at endogenic chaos and linear features. The non-water-ice materials have been suggested as hydrated sulfate salts [*McCord et al.*, 1999] and/or sulfuric acid [*Carlson et al.*, 1999]. Models for the ice+ocean system suggest sulfate concentrations ranging from ~30% [*Kargel*, 1991] to 10% or less [*McKinnon and Zolensky*, 2003; *Zolotov and Shock*, 2001]. Ice-shell salinities of a few percent could plausibly result from disequilibrium incorporation of oceanic salts into a thickening ice shell [*Spaun and Head*, 2001] or injection of salty ocean water into fractures that form at the base of the shell [*Pappalardo and Barr*, 2004].

[4] Motivated by the difficulty of explaining domes with diapirs from thermal convection in pure ice, *Pappalardo and Barr* [2004] suggested that the domes instead result from compositional density contrasts in a salty ice shell. This scenario is plausible but at present remains largely qualitative. To rigorously test whether compositional convection can produce pits and uplifts, the convection equations must be solved in the presence of salinity. Of particular interest is how the topography evolves in the presence of large viscosity contrasts, which is difficult to assess with simple approaches such as adopted by *Pappalardo and Barr* [2004]. Here we present 2D numerical simulations of thermo-compositional convection in Europa's icy shell to evaluate the effects of salinity on surface features.

2. Model and Methods

[5] By assuming an infinite Prandtl number and Boussinesq approximation for an incompressible material, the following equations (for continuity, momentum, energy, and salinity, respectively) govern the thermo-compositional convection in Europa's salty ice shell:

$$\nabla \cdot u = 0 \tag{1}$$

$$\nabla\sigma - \nabla p + f = 0 \tag{2}$$

$$\frac{\partial T}{\partial t} + u \cdot \nabla T = \kappa \nabla^2 T + q \tag{3}$$

$$\frac{\partial S}{\partial t} + u \cdot \nabla S = q_s \tag{4}$$

where u is velocity, σ is deviatoric stress tensor, p is dynamic pressure, f is the body force due to thermal and compositional buoyancy, T is temperature, t is time, $\kappa = 1 \times 10^{-6}$ m^2 s^{-1} is thermal diffusivity, q is internal heating, S is salinity, and q_s is the source and/or sink of salinity. Salinity diffusion is neglected, because it is much smaller than the thermal diffusion.

[6] In its most general form, f should also include a term associated with non-zero melt fractions. Because the permeability increases sharply with melt fraction [*Stevenson and Scott*, 1991], modest increases in melt fraction greatly increase the percolation rate, which tends to stabilize the melt fraction at small values of ~0.001–0.01 for conditions relevant to Europa (see equations given by *Showman et al.* [2004] and *Gaidos and Nimmo* [2000]). This produces density perturbations substantially smaller than that associated with the few percent salinity contrasts considered here. Therefore, we assume that the effect of melt on the density

[1]Department of Planetary Sciences, Lunar and Planetary Laboratory, University of Arizona, Tucson, Arizona, USA.
[2]Planetary Science Institute, Tucson, Arizona, USA.

0094-8276/05/2005GL023979$05.00

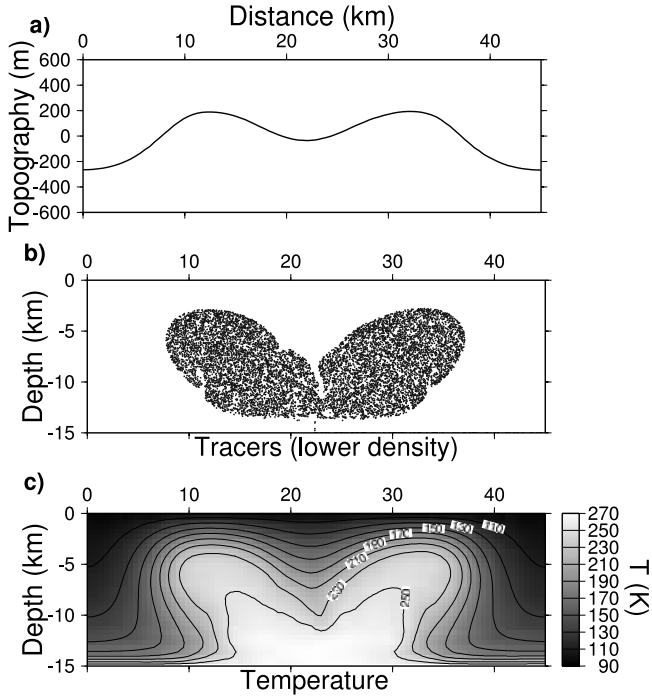

Figure 1. (a) Dynamic topography, (b) composition, and (c) temperature for a simulation in a domain 45 km wide and 15 km deep. The simulation has $\eta_0 = 10^{13}$ Pa·s, $\chi = 10^4$, and $\Delta\rho = 5\%$. The resulting topography has amplitude of 200–300 m and width of 15–20 km. The black particles in panel b represent the low-density ice.

can be neglected and that we can simply solve Equations (1)–(4) as written.

[7] In this paper, the temperature-dependent viscosity is implemented and defined as [*Showman and Han*, 2004]:

$$\eta(T)/\eta_0 = \min\left[\chi,\ \exp\left\{A\left(\frac{T_m}{T} - 1\right)\right\}\right] \qquad (5)$$

where T is temperature, $T_m = 270$ K, and $\eta_0 = 10^{13}$–10^{15} Pa·s is the viscosity at T_m, implying grain size of 0.1–1 mm. We adopt $A = 26$, corresponding to an activation energy of 60 kJ mol^{-1}. The cutoff viscosity contrast, χ, ranges from 10^4–10^7 and is intended as a crude representation of brittle rheology in Europa's ice shell. The effects of salt contamination on ice viscosity are poorly understood, but experiments show that the addition of hard particles to ice (a proxy for impurities) does not substantially affect the rheology for volume fractions less than ~10% [*Durham et al.*, 1992]. Premelting and partial melting may cause one order of magnitude decrease in viscosity [*De La Chapelle et al.*, 1999; *Tobie et al.*, 2003]. However, this value is modest compared with viscosity changes (10^4–10^7) due to temperature variations. So we neglect the viscosity changes due to salinity and partial melting.

[8] We use the Particle-In-Cell (PIC) finite element code Ellipsis [*Moresi et al.*, 2003] to solve the above equations in 2D cartesian geometry. The velocity boundary conditions are reflective on the sides and free-slip on the top and bottom. The bottom temperature is fixed at 270 K, and the top is held at 95 K. The initial temperature increases linearly from the top to the bottom with a small disturbance to trigger convection. The length to thickness ratio of the simulation domain is 3:1 or 6:1. We explore ice shell thicknesses of 5, 10, 15, and 30 km, consistent with predictions that Europa's ice shell thickness is less than 30 km [*Ojakangas and Stevenson*, 1989; *Tobie et al.*, 2003].

[9] Following *Pappalardo and Barr* [2004], and consistent with numerical convection simulations [*Tobie et al.*, 2003; *Showman and Han*, 2004], we envision that partial melting occurs most easily near the base of Europa's ice shell; segregation of salts into the melt and downward percolation of melt into the ocean promotes formation of relatively salt-free ice near the base of the shell. Accordingly, we initialize most simulations with a relatively salt-poor basal layer overlain by a denser, saltier layer. Density ranging from 950–1100 kg/m^3 and compositional density contrasts ($\Delta\rho$) ranging from 2–10% are explored, corresponding to salinities of ~3–15%, broadly consistent with available constraints [*Kargel*, 1991; *Zolotov and Shock*, 2001; *McKinnon and Zolensky*, 2003]. In some simulations we include a salinity sink wherever the temperature reaches the expected melting temperature. No salinity sources are included in these preliminary simulations.

3. Results

[10] Our simulations show that, for melting-temperature viscosity (η_0) of 10^{13} Pa·s and viscosity contrasts of $\leq 10^6$, uplifts and depressions with amplitude of 100–700 m can occur in an ice shell 10–30 km thick when the compositional density contrasts are ~2–10%. Figure 1 illustrates this phenomenon for a simulation with a thickness of 15 km and a viscosity contrast (χ) of 10^4; the simulation was initialized with a density of 1000 kg m^{-3} from 0–12 km depth and a density of 950 kg m^{-3} from 12–15 km depth (representing salty and relatively salt-free layers, respectively). In the simulation, the low-density material develops numerous small-scale (~few-km-wide) convective instabilities before ascending en masse into a 20 km-wide diapir, which splits in two as dense, salty ice descends through its center (Figure 1). The topography results from the horizontal buoyancy contrasts; the combined buoyancy from compositional and temperature variations far exceeds the thermal buoyancy alone, which explains why the topography far exceeds that obtained in earlier, pure-ice simulations [*Showman and Han*, 2004, 2005]. Eventually, the lower density material from the bottom mixes with the higher density material at the top, and the strong surface topography disappears.

[11] Similar behavior occurs when the initial ice shell is uniformly salty but salt removal is allowed for temperatures exceeding the expected melting temperature of low-eutectic-temperature contaminants such as hydrated chloride salts and sulfuric acid (Figure 2). Hydrated chlorides and sulfuric acid have eutectic temperatures of ~220–250 K and 211 K, respectively [*Kargel*, 1991]. Here, partial melting is assumed to begin at temperatures of 220 K, leading to a reduction in density of up to 5% due to salt loss as temperatures rise to 250 K or above. Temperature-dependent tidal heating is also used with a tidal-flexing amplitude of 10^{-5} [see *Showman and Han*, 2004, equation 7]. As tidal heating and thermal conduction from the bottom warm the interior of the ice shell above 220 K,

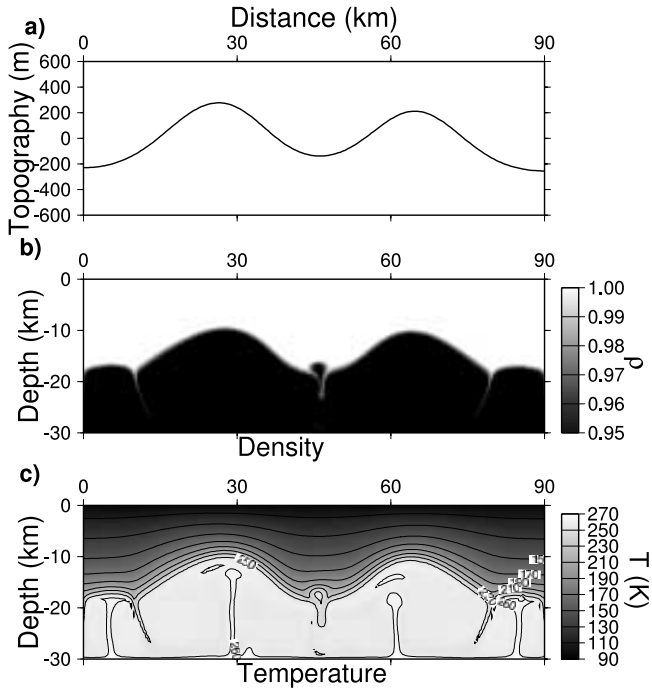

Figure 2. (a) Dynamic topography, (b) density, and (c) temperature for a simulation in a domain 90 km wide and 30 km deep. The simulation has $\eta_0 = 10^{13}$ Pa·s, $\chi = 10^5$. Partial melting is assumed to begin at temperatures of 220 K, leading to a reduction in density of up to 5% as temperatures rise to 250 K or above. The resulting topography has amplitude of 300–500 m and width of 30 km.

salt loss occurs, leading to a low-density layer near the bottom boundary. Thermal convection initiates within this layer (allowed by the small viscosity at these high temperatures), and the layer becomes relatively isothermal (Figure 2c). The stiff, salty ice at temperatures less than 220 K acts as a stagnant lid, which becomes Rayleigh-Taylor unstable relative to the underlying low-density ice. Perturbations in the interface between the salty lid and the underlying salt-poor ice (Figure 2b) amplify over time, eventually producing diapirs ~20 km wide. Uplifts and pits 300–500 m in amplitude, with diameters of 30 km, are produced on the surface (Figure 2a).

[12] Our simulations show that the formation time for pits and domes is approximately proportional to the surface viscosity (Figure 3). The pit/dome formation time is 10^4–10^5 years for a viscosity contrast of 10^4 (depending on ice-shell thickness) and increases to 10^6–10^7 years for a viscosity contrast of 10^6. This behavior can be qualitatively understood using arguments analogous to those given by *Whitehead* [1988, pp. 69–71]. For Rayleigh-Taylor instabilities with horizontal wavelengths comparable to the layer thickness (as occurs in our simulations), the growth timescale for the instability is $\sim\eta_0\chi/(g\delta\Delta\rho)$, where $\Delta\rho$ is the density difference across the interface between the salty and salt-poor layers and δ is the thickness of the salty layer. Adopting $\delta \approx d/2$, g = 1.3 m s^{-2}, and $\Delta\rho$ = 100 kg m^{-3} leads to growth timescales that agree with Figure 3 within an order of magnitude. The total lifespans of pits and domes are several times greater than the formation times shown in Figure 3.

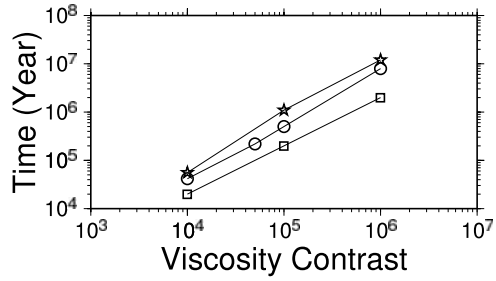

Figure 3. Pit/dome formation time versus viscosity contrast and thickness of ice shell. All the simulations use $\eta_0 = 10^{13}$ Pa·s and $\Delta\rho$ = 10%. Different symbols represent simulations with different ice shell thickness: Stars: thickness = 10 km. Circles: thickness = 15 km. Squares: thickness = 30 km. Formation time is proportional to viscosity contrast. Europa's surface age is 30–100 Myr.

[13] Nevertheless, our results (Figure 3) indicate that Europa's pits and uplifts cannot result from convection if the viscosity contrast exceeds $\sim 10^7$–10^8 (upper layer viscosity > 10^{20}–10^{21} Pa·s), because in this case the formation time for the topography would exceed Europa's known surface age of 30–100 Myr [*Zahnle et al.*, 2003]. The actual viscosity contrast associated with thermally activated viscous creep in Europa's ice shell is about 10^{10}–10^{20}. Therefore, compositional convection can only explain Europa's pits and uplifts if brittle processes weaken the surface layers, allowing brittle surface deformation over timescales less than Europa's surface age.

[14] Figure 4 summarizes the dependence of topographic amplitude on ice-shell thickness, viscosity contrast, and maximum compositional density variation from our simulations. The simulations were performed in ice shells 5–30 km thick, with 2–10% compositional density variation and 10^4–10^6 viscosity contrast. As expected, the dependence of topographic amplitude on viscosity contrast is weak. For a given viscosity contrast and maximum density variation, the topography increases with ice-shell thickness. Topography with amplitude of 100–700 m and width of 10–30 km can be produced in the simulations in an ice shell 10–30 km thick for density variations of 2–10% and viscosity contrasts of $\leq 10^6$.

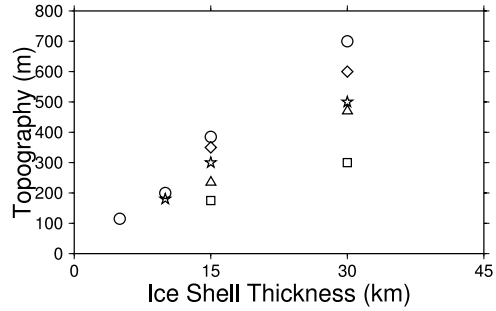

Figure 4. Topography of pits/uplifts versus density variation ($\Delta\rho$), viscosity contrast (χ), and thickness of ice shell. The simulations use $\eta_0 = 10^{13}$ Pa·s. Different symbols represent models with different parameters: Circles: $\Delta\rho$ = 10%, $\chi = 10^4$. Triangles: $\Delta\rho$ = 5%, $\chi = 10^4$. Squares: $\Delta\rho$ = 2%, $\chi = 10^4$. Diamonds: $\Delta\rho$ = 10%, $\chi = 10^5$. Stars: $\Delta\rho$ = 10%, $\chi = 10^6$.

[15] Interestingly, diapirism can produce pits and uplifts with heights of up to 100 m even in an ice shell as thin as 5 km, as long as the compositional density contrasts are large (10%) and the viscosity contrast is modest (10^4). Such thin shells have Rayleigh numbers less than the critical (thermal) Rayleigh number and are hence stable to purely thermal convection. However, the large compositional density contrasts and weak salinity diffusion make these shells *unstable* to overturning by *compositional* convection.

[16] The thickness of the basal salt-poor layer influences Europa's surface topography. Our simulations show that increasing the thickness of the salt-poor layer from 20% to 40% of the total shell thickness leads to an increase in the width of uplifts by a factor of ~2. Furthermore, our simulations show that the melting-temperature viscosity (η_0) impacts the amplitude and formation time (lifespan) of topography. By increasing η_0 from 10^{13} Pa·s to 10^{14} or 10^{15} Pa·s (at a constant ice-shell thickness), the topographic amplitude will decrease about 25% or 50%, respectively, and formation time (lifespan) becomes about 10 or 100 times longer.

4. Summary

[17] Thermo-compositional convection in Europa's icy shell can produce pits and domes under appropriate conditions. If the compositional density variation is 2–10% and the viscosity contrast is less than 10^6, thermo-compositional convection produces pits and uplifts with topographic amplitudes of 100–700 m and widths of 10–30 km in an ice shell 10–30 km thick. These results match the topographic amplitudes and widths of Europa's largest pits and uplifts. In our simulations, the widest structures generally form in the thickest shells and vice versa. Our simulations have difficulty explaining the many pits and uplifts with diameters <5 km [*Greenberg et al.*, 2003]. The viscosity structure strongly influences the pit/uplift formation time and lifespan; topography forms too slowly to explain Europa's pits and uplifts if the viscosity contrast exceeds 10^7–10^8. Conceivably, brittle behavior in the cold near-surface ice could allow the lithospheric deformation necessary for uplifts and pits to form [*Showman and Han*, 2005].

[18] Although the pits and uplifts in our simulations are transient features (especially at viscosity contrasts $<10^5$), it is possible that melt-filled fractures may continually inject salt into the ice shell and that partial melting near the base of the shell (perhaps driven by tidal heating) followed by downward melt percolation would produce a continuing supply of fresh, low-density ice there [*Pappalardo and Barr*, 2004]. Our future models will include these sources and sinks to determine whether pits and uplifts can be continually generated on Europa.

[19] **Acknowledgments.** This work was supported by grant NNG05GI14G from NASA's Outer Planets Research Program. We would like to thank Gabriel Tobie and an anonymous reviewer for their constructive reviews.

References

Carlson, R. W., R. E. Johnson, and M. S. Anderson (1999), Sulfuric acid on Europa and the radiolytic sulfur cycle, *Science*, *286*, 97–99.

Collins, G. C., J. W. Head, R. T. Pappalardo, and N. A. Spaun (2000), Evaluation of models for the formation of chaotic terrain on Europa, *J. Geophys. Res.*, *105*, 1709–1716.

De La Chapelle, S., H. Milsch, O. Castelnau, and P. Duval (1999), Compressive creep of ice containing a liquid intergranular phase: Rate-controlling processes in the dislocation creep regime, *Geophys. Res. Lett.*, *26*, 251–254.

Durham, W. B., S. H. Kirby, and L. A. Stern (1992), Effects of dispersed particulates on the rheology of water ice at planetary conditions, *J. Geophys. Res.*, *97*, 20,883–20,897.

Gaidos, E. J., and F. Nimmo (2000), Tectonics and water on Europa, *Nature*, *405*, 637.

Greeley, R., et al. (1998), Europa: Initial Galileo geological observations, *Icarus*, *135*, 4–24.

Greenberg, R., M. A. Leake, G. V. Hoppa, and B. R. Tufts (2003), Pits and uplifts on Europa, *Icarus*, *161*, 102–126.

Head, J. W., and R. T. Pappalardo (1999), Brine mobilization during lithospheric heating on Europa: Implications for formation of chaos terrain, lenticula texture, and color variations, *J. Geophys. Res.*, *104*, 27,143–27,155.

Kargel, J. S. (1991), Brine volcanism and the interior structures of asteroids and icy satellites, *Icarus*, *94*, 368–390.

McCord, T. B., et al. (1999), Hydrated salt minerals on Europa's surface from the Galileo near-infrared mapping spectrometer (NIMS) investigation, *J. Geophys. Res.*, *104*, 11,827–11,851.

McKinnon, W. B., and M. E. Zolensky (2003), Sulfate content of Europa's ocean and shell: Evolutionary considerations and some geological and astrobiological implications, *Astrobiology*, *3*(4), 879–897.

Moresi, L., F. Dufour, and H. B. Muhlhaus (2003), A Lagrangian integration point finite element method for large deformation modeling of viscoelastic geomaterials, *J. Comput. Phys.*, *184*, 476–497.

Nimmo, F., and M. Manga (2002), Causes, characteristics, and consequences of convective diapirism on Europa, *Geophys. Res. Lett.*, *29*(23), 2109, doi:10.1029/2002GL015754.

Ojakangas, G. W., and D. J. Stevenson (1989), Thermal state of an ice shell on Europa, *Icarus*, *81*, 220–241.

Pappalardo, R. T., and A. C. Barr (2004), The origin of domes on Europa: the role of thermally induced compositional diapirism, *Geophys. Res. Lett.*, *31*, L01701, doi:10.1029/2003GL019202.

Pappalardo, R. T., et al. (1998), Geological evidence for solid-state convection in Europa's ice shell, *Nature*, *391*, 365–368.

Rathbun, J. A., G. S. Musser, and S. W. Squyres (1998), Ice diapirs on Europa: Implications for liquid water, *Geophys. Res. Lett.*, *25*, 4157–4160.

Riley, J., G. V. Hoppa, R. Greenberg, B. R. Tufts, and P. Geissler (2000), Distribution of chaotic terrain on Europa, *J. Geophys. Res.*, *105*, 22,599–22,615.

Showman, A. P., and L. Han (2004), Numerical simulations of convection in Europa's ice shell: Implications for surface features, *J. Geophys. Res.*, *109*, E01010, doi:10.1029/2003JE002103.

Showman, A. P., and L. Han (2005), Effects of plasticity on convection in an ice shell: Implications for Europa, *Icarus*, *177*(2), 425–437.

Showman, A. P., I. Mosqueira, and J. W. Head (2004), On the resurfacing of Ganymede by liquid-water volcanism, *Icarus*, *172*, 625–640.

Sotin, C., J. W. Head, and G. Tobie (2002), Europa: Tidal heating of upwelling thermal plumes and the origin of lenticulae and chaos melting, *Geophys. Res. Lett.*, *29*(8), 1233, doi:10.1029/2001GL013844.

Spaun, N. A., and J. W. Head (2001), A model of Europa's crustal structure: Recent Galileo results and implications for an ocean, *J. Geophys. Res.*, *106*, 7567–7576.

Stevenson, D. J., and D. R. Scott (1991), Mechanics of fluid-rock systems, *Annu. Rev. Fluid Mech.*, *23*, 305–339.

Tobie, G., G. Choblet, and C. Sotin (2003), Tidally heated convection: constraints on Europa's ice shell thickness, *J. Geophys. Res.*, *108*(E11), 5124, doi:10.1029/2003JE002099.

Whitehead, J. A. (1988), Fluid models of geological hotspots, *Annu. Rev. Fluid Mech.*, *20*, 61–87.

Zahnle, K., P. Schenk, H. F. Levison, and L. Dones (2003), Cratering rates in the outer solar system, *Icarus*, *163*, 263–289.

Zolotov, M. Y., and E. L. Shock (2001), Composition and stability of salts on the surface of Europa and their oceanic origin, *J. Geophys. Res.*, *106*, 32,815–32,827.

L. Han and A. P. Showman, Department of Planetary Sciences, Lunar and Planetary Laboratory, University of Arizona, Tucson, AZ 85721, USA. (lhan@lpl.arizona.edu)